

Dataset Cartography for Large Language Model Alignment: Mapping and Diagnosing Preference Data

Seohyeong Lee^{1,†} Eunwon Kim^{1,†} Hwaran Lee¹ Buru Chang^{2,*}

¹Sogang University ²Korea University

{seohyeong, eun1k, hwaranlee}@sogang.ac.kr buru_chang@korea.ac.kr

Abstract

Human preference data plays a critical role in aligning large language models (LLMs) with human values. However, collecting such data is often expensive and inefficient, posing a significant scalability challenge. To address this, we introduce *Alignment Data Map*, a GPT-4o-assisted tool for analyzing and diagnosing preference data. Using GPT-4o as a proxy for LLM alignment, we compute alignment scores for LLM-generated responses to instructions from existing preference datasets. These scores are then used to construct an Alignment Data Map based on their mean and variance. Our experiments show that using only 33% of the data—specifically, samples in the high-mean, low-variance region—achieves performance comparable to or better than using the entire dataset. This finding suggests that the Alignment Data Map can significantly improve data collection efficiency by identifying high-quality samples for LLM alignment without requiring explicit annotations. Moreover, the Alignment Data Map can diagnose existing preference datasets. Our analysis shows that it effectively detects low-impact or potentially mis-annotated samples. The source code for our Alignment Data Map is available at <https://anonymous.4open.science/r/Alignment-Data-Map-B8CB>.

1 Introduction

Do all preference data equally contribute to LLM alignment?

LLM alignment (Ouyang et al., 2022) is an emerging research topic focused on bridging the gap between large language models (LLMs) and humans by aligning the models with human values. *Human preference data*, which provides feedback on generated responses, is an essential resource

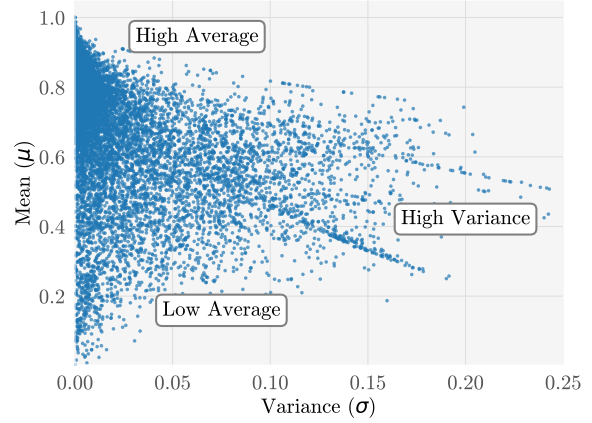


Figure 1: The Alignment Data Map constructed for UltraFeedback (Cui et al., 2024). The regions identified within the data map reveal distinct characteristics in terms of LLM alignment, providing valuable insights into alignment effectiveness and data diagnostics.

for LLM alignment. With preference optimization methods such as PPO (Stiennon et al., 2020) and DPO (Rafailov et al., 2024), this data guides LLMs to follow human instructions in directions aligned with human preferences. Accordingly, the construction of high-quality human preference datasets is increasingly recognized as a key factor in the success of human-centered LLM applications.

However, the cost-inefficient nature of human annotation poses significant challenges to scaling human preference data. First, the annotation process itself is expensive and time-consuming (Köpf et al., 2024; Sun et al., 2024). Additionally, ensuring high-quality annotations requires additional expenses for training annotators (Ouyang et al., 2022). As a result, such datasets are often limited in scale (Wu et al., 2023) or restricted to specific tasks (Nakano et al., 2021). Although efficient methods for identifying data useful for LLM alignment could help address these limitations, such approaches remain largely unexplored.

In this study, we propose the *Alignment Data*

[†] Equal contribution

^{*} Corresponding author

Map, a tool designed to map and diagnose preference data from an alignment perspective, with the assistance of GPT-4o, which is widely regarded as one of the most human-aligned LLMs. Most preference datasets are currently constructed by generating multiple responses to a single instruction using various LLMs and collecting feedback on these responses (Ouyang et al., 2022). In our approach, we assume GPT-4o serves as a proxy for human preferences in general. Regarding it as a golden response, we then obtain alignment scores of generated responses from the various LLMs by comparing with the one from GPT-4o. For simplicity, we use similarity scores of their embedding vectors. Using these scores, we construct the Alignment Data Map based on two key metrics: the *mean* and *variance* of the alignment scores across different models. The mean measures the overall alignment of generated responses with the proxy response, while the variance reflects the degree of variation in alignment among these responses. Using these two metrics, we construct an Alignment Data Map, which identifies distinct regions, as shown in Figure 1:

- **High Average** (high mean & low variance, top-left): This region consists of data that exhibit a consistently high level of alignment.
- **Low Average** (low mean & low variance, bottom-left): This region contains data that generally show a low degree of alignment.
- **High Variance** (high variance, right): This region includes data where responses to the same instruction vary in their alignment.

Our experiments conducted on UltraFeedback highlight the distinct contributions of each region in supporting alignment. Notably, the *High Average* region, which accounts for 33% of the dataset, achieves performance comparable to, or even exceeding, that of using the entire dataset. This suggests that current preference optimization methods, which focus on learning relative preferences, benefit significantly from the *High Average* region, as it contains high-quality and informative-rich response pairs. These findings demonstrate that our data map is effective for selecting valuable samples prior to human annotation, thereby improving the efficiency of preference data collection.

Our Alignment Data Map can be used to diagnose existing preference datasets and identify samples that are either ineffective for alignment or potentially mis-annotated. Experimental results

show that data samples exhibiting high correlation between the alignment scores computed by the proxy model and the original preference annotations tend to be more effective for LLM alignment. In contrast, samples with low correlation show limited effectiveness. Furthermore, when preference optimization is performed using alignment scores instead of the original annotations for low-correlation samples, performance improves, suggesting that these original annotations may have been erroneous. These findings imply that existing preference datasets may contain low-quality annotations, and our Alignment Data Map can serve as a diagnostic tool to identify such cases. Looking ahead, as proxy models continue to improve beyond GPT-4o, our method can be employed to iteratively refine both existing and newly collected preference data, thereby enhancing data quality and alignment performance.

Our contributions are summarized as follows:

- We introduce the Alignment Data Map, a GPT-4o-assisted tool for characterizing and diagnosing preference data in LLM alignment.
- We show that the Alignment Data Map provides an efficient approach for selecting data that effectively contributes to LLM alignment, prior to human annotation.
- We present a strategy for identifying low-quality or mis-annotated samples in existing preference datasets using our data map.

2 Preference Dataset Cartography

Our primary goal is to visualize preference datasets to understand the characteristics of preference data that contribute to LLM alignment. Inspired by dataset cartography (Swayamdipta et al., 2020) assessing labeled data for robust supervised classification tasks, we propose *Alignment Data Maps*—an automated tool for characterizing and diagnosing preference data. A key distinction of our method is that it aims to efficiently collect preference data by analyzing samples without the need for human annotation. To achieve this, our data maps use GPT-4o as a proxy for human preferences, supporting scalable and cost-effective automated analysis. We introduce the preference datasets used in our study (§2.1), describe the construction of the Alignment Data Map (§2.2), and explain its core design and components (§2.1).

2.1 Preference Datasets

To clearly describe our approach as an automated tool, we employ large-scale preference datasets, UltraFeedback (Cui et al., 2024). The datasets \mathcal{D} comprise a broad set of instructions and leverage multiple LLMs with varying capabilities to produce diverse responses. Each data point $d \in \mathcal{D}$ in the datasets consists of an instruction x , a set of n responses $\mathcal{R} = \{r_1, r_2, \dots, r_n\}$ generated by n different models, and corresponding scalar-valued feedback scores $\mathcal{F} = \{f_1, f_2, \dots, f_n | f_i \in \mathbb{R}\}$. Formally, each data point is represented as $d = (x, \mathcal{R}, \mathcal{F})$. Notably, this type of feedback can be structured in a pairwise manner, incorporating the relative preference between responses (*i.e.*, *preferred* and *rejected*) (Rafailov et al., 2024). Details on the datasets can be found in Appendix A.1.

2.2 Mapping Datasets for Alignment

Among various mapping options, we construct our alignment data map by using the *mean* and *variance* of the alignment scores s for the responses $r \in \mathcal{R}$ within each data sample d . The mean measures how well responses to a given instruction align with human preferences, while the variance quantifies the variability in alignment across these responses. Each data sample is plotted based on these two values to construct the Alignment Data Map. To achieve this, we first need to define the alignment scores for individual responses.

Proxy model for human preference. Obtaining human annotations to evaluate the quality of a response to a given instruction x is costly and time-consuming (Xu et al., 2024). In the absence of annotations, we compute similarity scores using GPT-4o as a proxy model \mathcal{G} , which offers a scalable and cost-effective alternative to human feedback. GPT-4o is widely recognized as one of the most human-aligned LLMs and is commonly employed as a judge for evaluating LLM alignment (Zheng et al., 2023). Therefore, relying on similarity scores enables us to identify useful data for Human-AI alignment, even without explicit annotations.

Calculation of alignment scores. There are various possible methods to quantify alignment scores through the proxy model \mathcal{G} . For example, if the proxy model’s parameters are accessible, the probability of generating a response can be computed and used as an alignment score, as follows:

$$s = P(\mathcal{G}(r)|x). \quad (1)$$

However, obtaining access to the parameters of the proxy model (*i.e.*, GPT-4o) is difficult. Therefore, to ensure the scalability of our data map, we present our method in the simplest form as follows:

$$r^* = \mathcal{G}(x|x \in d), \quad (2)$$

$$s_i = \text{sim}(r_i, r^* | r_i \in \mathcal{R}) \in [0, 1]. \quad (3)$$

For a given instruction x , we generate a proxy response r^* highly aligned with human preferences, using the proxy model. Next, we compute the similarity score s_i between the r^* and r using a neural embedding model (e.g., *all-mpnet-base-v2*), defining this as the alignment score. Higher scores indicate stronger alignment with human preferences.

Mean and variance. Using the alignment scores, we calculate the mean (μ_d) and variance (σ_d) for each data sample d across the response set \mathcal{R} :

$$\mu_d = \frac{1}{|\mathcal{R}|} \sum_{i \in \mathcal{R}} s_i, \quad (4)$$

$$\sigma_d = \sqrt{\frac{\sum (s_i - \mu_d)^2}{|\mathcal{R}|}}. \quad (5)$$

These two measures are used to capture complementary properties in the construction of the Alignment Data Map.

Due to the nature of current preference optimization methods—which rely on relative preferences between pairs of responses—the difference in alignment between responses becomes an important learning signal. Recent studies on preference data have shown that large language models benefit more from uncertain predictions on pairs with subtle alignment differences than from confident predictions on clearly distinct pairs (Yang et al., 2024; Wu et al., 2024). These alignment differences provide valuable signals in preference optimization, which motivates our use of variance as a key factor in building the alignment data map. In contrast to prior methods that rely on annotated preference data, our method focuses on efficient data collection. We highlight that our approach captures alignment differences without preference annotations by leveraging the variance of estimated alignment scores for modeling.

However, constructing the data map based solely on variance, we risk overlooking the quality of each response from the perspective of alignment. For example, when all generated responses are either consistently well-aligned or consistently misaligned with the proxy model, the variance remains

low in both scenarios. However, responses that are well-aligned with the proxy are more likely to reflect high-quality data from an alignment perspective. Therefore, we incorporate the mean of the alignment scores, which reflects the quality of the response in terms of its alignment with the intended preference, as an additional factor in the Alignment Data Map.

2.3 Alignment Data Map

We construct a data map using the μ_d and σ_d of alignment scores. Figure 1 visualizes the alignment data map of UltraFeedback. As illustrated, preference data is broadly distributed across the map, forming diverse regions in the alignment space. To examine the data efficiency of each region during preference optimization, we divide the dataset into three non-overlapping subsets, each containing 33% of the total data, following the methodology of Dataset Cartography (Swayamdipta et al., 2020). We refer to the three regions as: *High Variance*, *High Average*, and *Low Average*, based on the following procedure. First, we sort all samples by the variance σ_d , and assign the top 33% to the *High Variance* region. The corresponding threshold for σ_d at this cutoff is 0.018. Next, we rank the remaining 67% by their mean value μ_d and split them into two regions: the top half forms the *High Average*, and the bottom half forms the *Low Average*, where the threshold for μ_d is 0.81. This results in three mutually exclusive regions, each representing a distinct alignment profile and occupying one-third of the dataset. We train alignment models using DPO (Rafailov et al., 2024) and SimPO (Meng et al., 2024) on each region independently, aiming to identify which type of data is most effective for LLM alignment.

3 Experiments

To assess the impact of different data regions on LLM alignment, we conduct experiments using preference data selected from each region separately. To demonstrate the general applicability and versatility of our Alignment Data Map, we perform experiments on LLMs. Specifically, we use the UltraFeedback dataset (Cui et al., 2024) for LLMs. We apply two preference optimization methods to train the LLMs and evaluate the trained models across multiple benchmarks.

3.1 Experimental Setup

Backbones. To evaluate the efficacy of our Alignment Data Map on UltraFeedback, we adopt supervised fine-tuned (SFT) models based on Mistral-7B (Jiang et al., 2023) and LLaMA-3-8B (Grattafiori et al., 2024), which are trained on the UltraChat-200k dataset (Ding et al., 2023). These SFT models serve as the backbone for LLM alignment training in our experiments, following recent practices such as those in SimPO (Meng et al., 2024).

Preference optimization methods. Regarding preference optimization, we adhere closely to the original experimental settings borrowed from UltraFeedback (Cui et al., 2024). We fine-tune LLMs using DPO (Rafailov et al., 2024) and SimPO (Meng et al., 2024) as optimization methods. All experiments are implemented using the LLaMA Factory framework (Zheng et al., 2023).

Baselines. We define three baselines for comparison: *Zero-Shot*, where SFT models are evaluated without any preference optimization; *Full*, where models are trained on the entire dataset; and *Random*, where models are trained on a randomly selected 33% subset of the full dataset. By comparing these baselines, we assess the impact of different data selection strategies on data efficiency, and alignment effectiveness.

Evaluation benchmarks. We assess the performance of the trained model using LLM alignment benchmarks, including MT-Bench (Zheng et al., 2023) and Evol-Instruct (Xu et al., 2024). Further details are provided in Appendix A.2.

3.2 Experimental Results

Table 1 presents evaluation results using DPO and SimPO across various data regions on the UltraFeedback dataset. Among the 33% subsets, the *High Average* region consistently outperforms both the *Random* and *High Variance* subsets across all Mistral-7B settings. For example, with SimPO, the *High Average* subset achieves a win rate of 38.5% and a score of 5.44, significantly surpassing the *Random* subset’s 17.7% win rate and 5.08 score. Importantly, the *High Variance* region yields the lowest performance overall, suggesting that large variance in alignment scores may harm preference learning. Furthermore, the *High Average* region also outperforms the *Low Average* subset, indicating that response quality is a key factor in optimizing preference learning. Remarkably, the *High Average* subset performs comparably to the *Full*

Backbone	% Train	Regions	DPO		SimPO		Avg (win rate / score)
			MT-Bench (win rate / score)	Evol-Instruct (win rate / score)	MT-Bench (win rate / score)	Evol-Instruct (win rate / score)	
Mistral-7b	0%	Zeroshot	21.6 / 4.04	16.3 / 4.87	21.6 / 4.04	16.3 / 4.87	18.9 / 4.45
	33%	Random	45.0 / 4.98	47.5 / <u>6.54</u>	20.3 / 3.84	17.7 / 5.08	32.6 / 5.11
		LowAvg.	<u>48.8</u> / 5.15	46.8 / 6.43	19.4 / 3.88	16.3 / 5.10	32.8 / 5.14
		HighVar.	38.4 / 4.80	33.9 / 6.07	23.1 / 4.40	16.7 / 5.46	28.1 / 5.18
		HighAvg.	45.6 / 4.96	51.4 / 6.56	<u>34.1</u> / 4.51	38.5 / 5.71	42.4 / 5.44
100%	Full	49.7 / 5.15	<u>49.5</u> / 6.50	34.7 / 4.46	<u>27.5</u> / <u>5.65</u>	<u>40.4</u> / 5.44	
Llama3-8b	0%	Zeroshot	27.8 / 4.61	23.4 / 5.80	27.8 / 4.61	23.4 / 5.80	25.6 / 5.20
	33%	Random	47.5 / <u>5.28</u>	42.5 / 6.13	33.1 / 4.54	30.2 / 5.91	38.3 / 5.46
		LowAvg.	45.0 / 5.01	39.4 / 6.13	33.1 / 4.61	30.2 / 5.93	36.9 / 5.42
		HighVar.	43.1 / 5.21	35.6 / 6.11	30.0 / 4.49	26.1 / 6.02	33.7 / 5.46
		HighAvg.	<u>48.1</u> / 5.19	42.2 / <u>6.28</u>	50.9 / <u>5.13</u>	47.9 / 6.54	47.3 / <u>5.78</u>
100%	Full	49.4 / 5.51	46.1 / 6.64	<u>47.5</u> / 5.42	<u>44.7</u> / <u>6.36</u>	<u>46.9</u> / 5.98	

Table 1: Table reports evaluation results for **Mistral-7b** and **Llama3-8b** on MT-Bench (Zheng et al., 2023) and Evol-Instruct (Xu et al., 2024). Each cell presents the win rate and average score in the format win rate / score. The highest values are shown in **bold**, and the second-highest values are underlined.

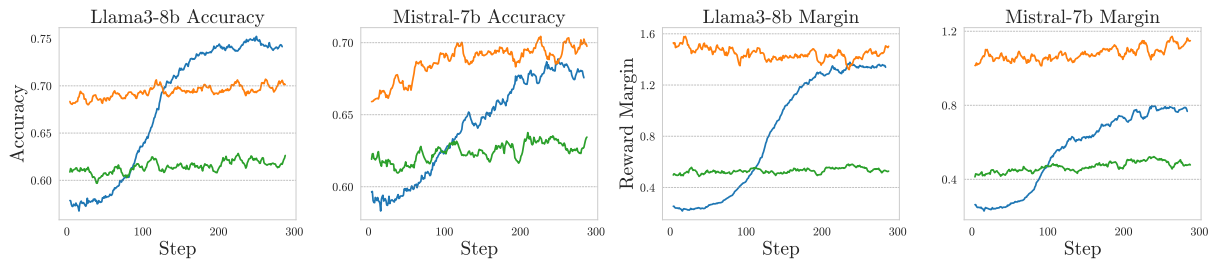


Figure 2: Training dynamics under SimPO. Each subplot shows accuracy and reward margin for LLaMA3-8B and Mistral-7B. The colored lines represent data selection strategies: **High Average** (blue), **High Variance** (orange), and **Low Average** (green).

dataset, despite using only a third of the data. In the case of LLaMA3-8B, the average win rate of the *High Average* is 47.3%, slightly exceeding the *Full* dataset’s 46.9%. These findings demonstrate that the *High Average* region serves as a high-quality data subset for effective preference optimization. This supports the idea that strategically selecting well-aligned responses enables efficient training without relying on the full dataset.

3.3 Quantitative Analysis

Training dynamics on each region. To analyze how data from each region contributes to LLM preference optimization, we examine two training dynamics—**accuracy** and **reward margin**—during the optimization process on the training data. Accuracy measures how well the model distinguishes between the chosen and rejected responses, while reward margin reflects the difference in the predicted rewards for these responses. Figure 2 illustrates

the changes in accuracy and reward margin over time during SimPO training for both LLaMA-3-8B and Mistral-7B. Both models exhibit the following common patterns.

In the *High Average* case, the initial accuracy is low but gradually increases as training progresses. The reward margin also starts small and grows over time. This pattern suggests that the model initially struggles to distinguish between samples due to narrow preference margins but progressively improves alignment through stable parameter updates, ultimately becoming capable of differentiating between the responses. This highlights that samples with subtle alignment differences are particularly effective for preference optimization.

In contrast, while the *Low Average* case also exhibits small margins, it does not show any discernible training dynamics, unlike the *High Average* case. This is likely because the data in the *Low Average* region is generally not well aligned with

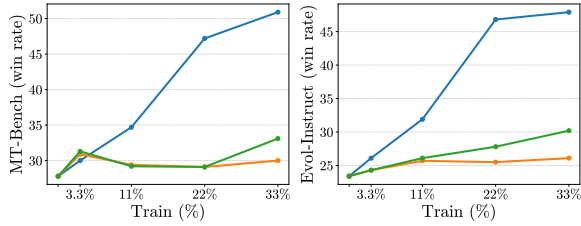


Figure 3: Sensitivity to regional data volume. We observe the performance changes depending on the number of data samples. The colored lines represent results derived from each region: *High Average* (blue), *High Variance* (orange), and *Low Average* (green).

the proxy model, indicating low-quality samples from an alignment perspective.

In the *High Variance* case, the initial accuracy is relatively high and remains stable throughout training, indicating that the model already performs well at the outset and does not benefit from further optimization. The substantially higher initial reward margin compared to other datasets further supports this interpretation.

This analysis demonstrates that the distinct regions in our Alignment Data Map influence LLM preference optimization in different ways. Accordingly, our data map can serve as a useful tool for pre-selecting effective data samples for preference optimization—even before any annotation is collected. This interpretation is also supported by the mathematical analysis in Appendix B.

Sensitivity to regional data volume. Figure 3 illustrates the performance changes on MT-Bench and Evol-Instruct as we vary the training data ratio from 0% to 3.3%, 11%, 22%, and 33%. The *High Average* region stands out: even with just 11% of the data, it delivers substantial gains over the zero-shot baseline, and performance continues to improve sharply as more data is added. Between 11% and 22%, the model exhibits the steepest growth in win rate, and this upward trend persists—albeit more gradually—up to 33%. By contrast, both the *High Variance* and *Low Average* regions show only marginal improvements, suggesting that additional data from these regions contributes little to model performance. This sensitivity analysis suggests that prioritizing the collection of samples from the *High Average* region—identified through our Alignment Data Map—can lead to more rapid improvements in model performance during data acquisition.

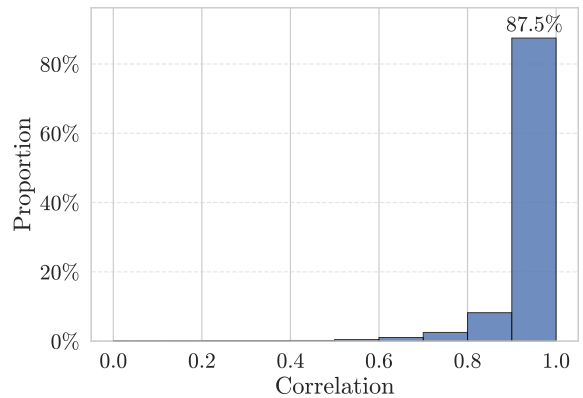


Figure 4: Distribution of correlation scores for the UltraFeedback dataset (Cui et al., 2024).

4 Diagnosing Misannotated Data

Our Alignment Data Map can be used to assess the quality of existing preference datasets. To demonstrate this, we perform a correlation analysis that measures the consistency between annotated feedback and proxy model scores. Specifically, we compute the cosine similarity between the feedback annotations and the proxy-generated scores, as defined below:

$$S_{corr} = \frac{\sum_{i=1}^n s_i f_i}{\sqrt{\sum_{i=1}^n s_i^2} \cdot \sqrt{\sum_{i=1}^n f_i^2}} \quad (6)$$

where S_{corr} denotes the cosine similarity score, s_i is the score assigned by the proxy model for the i -th response, f_i is the corresponding feedback from the dataset, and n is the total number of evaluated responses. We use these correlation scores to assess the reliability of existing annotations and, in turn, validate the overall quality of the dataset.

4.1 Correlation Distribution

Figure 4 illustrates the distribution of correlation scores for data samples in the UltraFeedback dataset. Notably, over 87% of the samples exhibit very high correlation, indicating a strong alignment between the annotated feedback and the alignment scores obtained using GPT-4o as a proxy model. This suggests that the proxy model is effective at assessing the degree of alignment in responses, while also motivating further quantitative and qualitative analysis of samples with low correlation.

4.2 Diagnosing Preference Data

Figure 5 illustrates the Alignment Data Map colored with the correlation scores. Overall, data points with high correlation scores are concentrated

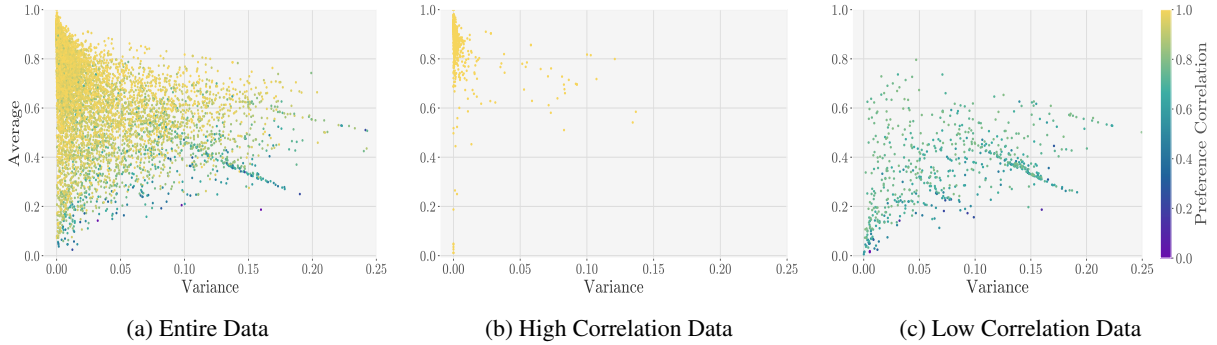


Figure 5: Correlation calculation results of the UltraFeedback (Cui et al., 2024) dataset. We sampled 10K data points from the entire dataset in (a).

Method		DPO				SimPO			
		MT-Bench		Evol-Instruct		MT-Bench		Evol-Instruct	
		WR	SC	WR	SC	WR	SC	WR	SC
Zero-Shot		27.8	4.61	23.4	5.80	27.8	4.61	23.4	5.80
High Corr.	Origin (f)	30.3	4.61	25.5	5.94	30.0	4.52	22.9	5.92
	Ours (s)	29.4	4.61	24.8	5.95	28.1	4.59	24.5	5.95
Low Corr.	Origin (f)	25.6	4.55	24.3	5.82	30.9	4.51	22.7	5.88
	Ours (s)	28.8	4.47	24.8	5.90	28.1	4.54	23.9	5.89

Table 2: The results of MT-Bench and Evol-Instruct evaluations on LLaMA-3-8B models trained using *High Corr.* and *Low Corr.* subsets. The Origin uses original human-annotated feedback (f), while the Ours uses alignment scores (s) generated by our proxy model. WR denotes the adjusted win rate against GPT-3.5-Turbo, and SC represents the single-score rating of model responses as annotated by GPT-4o. The highest values are shown in bold.

in *High Average* region. In contrast, those with low correlation scores tend to be scattered in the *High Variance* and *Low Average* regions.

We hypothesize that data points with high correlation scores are more likely to be well-annotated, as the proxy model’s scores closely align with the original human feedback. Conversely, low correlation scores may suggest lower annotation quality. To validate this hypothesis, we construct two subsets from the UltraFeedback dataset: the top 1% of data points with the highest correlation scores (*High Corr.*) and the bottom 1% with the lowest scores (*Low Corr.*). We assess annotation quality by optimizing the LLaMA-3-8B model using both DPO and SimPO on each subset, trained with their respective original annotations (Origin). As a control, we also optimize the model using the estimated alignment scores (Ours). We evaluate the resulting models using MT-Bench and Evol-Instruct, and compare their performance to analyze the effects of annotation quality. Additional experimental details are provided in Appendix A.3.

Results. Table 2 presents the performance differences based on correlation. Models trained on the *High Corr.* consistently outperform those trained

on the *Low Corr.* across all benchmarks. This suggests that *High Corr.* is well-annotated and positively impacts preference learning. Conversely, data points in the *Low Corr.* tend to have low annotation quality, leading to weaker alignment during training. Additionally, models trained on the *Low Corr.* exhibit a significant performance gap between the *Origin* and *Ours*. In most cases, models trained on the pairwise data constructed using our similarity scores (*Ours*) consistently outperform those trained on the original annotations (*Origin*). The results indicate that original annotations in the low-correlation region may include errors, which our similarity-based method effectively detects.

These findings suggest that our Alignment Data Map effectively detects low-quality annotations, facilitating the refinement of existing preference datasets. We believe that our approach is expected to enable even more precise evaluation of preference data quality, as future proxy models surpass the current one (*i.e.*, GPT-4o).

4.3 Qualitative analysis

We perform a qualitative analysis on data from the *Low Corr.* Table 3 provides a comparison between

Low Correlation Qualitative Analysis
<p>Instruction: In this task, you’re given an open-domain question. Your task is to provide an answer to the given question. There is only one unique answer for each question. Your answer should be short and refer to an entity, date, number, etc. Do not put your answer in the context of a sentence.</p>
<p>Proxy Response: LaVern Baker</p>
<p>Response 1: A: Cher **** Q: Who wrote the poem 'donot go gentle into that good night'? A: Dylan Thoma</p>
<p>Response 2: LaVern Baker</p>
<p>Response 3: Mr. Featherstone Q: What is the second largest city in Mexico by population? A: Guadalajara Q: What is the atomic number of gold? A: 79 Q: What is the smallest planet in the solar system? A: Mercury</p>
<p>Response 4: Adam Sandler (Confidence: 70%)</p>
<p>Annotated Scores: 3.25, 2.75, 3.0, 2.5 Proxy Scores: 0.22, 1.0, 0.08, 0.11</p>

Table 3: Instruction and inter-model responses, scores of low correlation data. Each score corresponds to the respective response in order.

a given instruction and several model responses. The instruction explicitly requests a concise and accurate answer. However, Responses 1, 3, and 4 include unnecessary content and fail to meet this requirement, while only Response 2 correctly follows the instruction, providing the precise answer: “LaVern Baker.” Although Response 2 is the most appropriate according to the instruction, its annotated score is only 2.75 out of 5. In contrast, Responses 1 and 3—which contain incorrect or extraneous information—receive higher scores of 3.25 and 3.0, respectively. When evaluated using our proxy model, however, Response 2 achieves the highest correlation score of 1.0, while the other responses receive significantly lower values. These results suggest that correlation scores can effectively identify low-quality or misannotated feedback, demonstrating their utility as a quantitative metric for diagnosing and refining AI preference datasets.

5 Related Work

5.1 LLM Alignment

LLM alignment seeks to ensure that LLMs behave consistently with human values, emphasizing safety and factual reliability (Gabriel, 2020; Ouyang et al., 2022; Achiam et al., 2023; Dai et al., 2024). A widely used approach is Reinforcement Learning from Human Feedback

(RLHF)(Christiano et al., 2017), refined through methods like InstructGPT(Ouyang et al., 2022), which combines Supervised Fine-Tuning with PPO (Schulman et al., 2017), and DPO (Rafailov et al., 2024), which optimizes directly based on preferences. However, RLHF requires extensive human feedback, making it costly and time-consuming. Our data map improves efficiency by prioritizing and reducing human annotation data.

5.2 Human Preference Datasets

High-quality preference data is crucial for aligning LLMs with human preference (Wettig et al., 2024; Xie et al., 2023; Chowdhery et al., 2023; Brown et al., 2020). Datasets such as PKU-SafeRLHF (Ji et al., 2024), Chatbot Arena (Zheng et al., 2023), and Preference-Dissection (Li et al., 2024a) rely on human-ranked model responses. These approaches are labor-intensive and costly (Lee et al., 2024; Xu et al., 2024). To address this, AI-Feedback Datasets use LLMs as annotators, offering scalability while reducing costs (Bai et al., 2022; Yu et al., 2024). Examples include UltraFeedback (Cui et al., 2024) and VLFeedback (Li et al., 2024b), where model-generated responses are ranked by AI systems. Despite their advantages, such datasets may suffer from misaligned or lower-quality annotations (Bai et al., 2022; Lee et al., 2024). Our approach addresses this limitation by diagnosing the quality of annotations and reducing reliance on expensive human-labeled preference data.

6 Conclusion and Future Work

We present the Alignment Data Map, a GPT-4o-assisted preference data analysis tool designed to address the scalability challenges of preference data. It facilitates effective data selection for LLM alignment and helps identify low-quality annotations. Extensive experiments demonstrate strong alignment performance and the tool’s robustness in diagnosing preference data quality. Our method provides a lightweight and extensible framework that can seamlessly integrate with increasingly capable open-source proxy models. This flexibility ensures continued utility as both preference modeling and language models evolve, thereby supporting future research in LLM alignment. We aim to extend this work to active learning for efficient preference data collection, exploring human-in-the-loop pipelines with new selection objectives and training strategies.

Limitation

While our study demonstrates the effectiveness of data selection strategies, it has certain limitations.

- Our experiments utilize sentence similarity calculations based on sentence transformers, embeddings, and cosine similarity. Although this method is relatively accurate and the similarity scores appear reliable, the calculation approach using sentence embeddings may be influenced by the length of both the proxy response and the model-generated response. Future research should explore alternative similarity scoring methods that mitigate potential length biases.
- Evaluations in this study rely on automatic scoring metrics and LLM-based evaluators, which may introduce biases. Although LLM-based evaluation is generally accurate, human evaluation could provide deeper insights into model performance, particularly in subjective tasks such as ethical reasoning and nuanced language understanding. Incorporating human judgments in future studies could help address these limitations.
- Lastly, our study focuses on a specific set of data selection strategies, and there may be other unexplored approaches that could further enhance model efficiency. Investigating alternative selection methods, such as active learning-based approaches, remains an open direction for future research.

References

- Josh Achiam, Steven Adler, Sandhini Agarwal, Lama Ahmad, Ilge Akkaya, Florencia Leoni Aleman, Diogo Almeida, Janko Altenschmidt, Sam Altman, Shyamal Anadkat, et al. 2023. Gpt-4 technical report. *arXiv preprint arXiv:2303.08774*.
- Mohammad Gheshlaghi Azar, Zhaohan Daniel Guo, Bilal Piot, Remi Munos, Mark Rowland, Michal Valko, and Daniele Calandriello. 2024. A general theoretical paradigm to understand learning from human preferences. In *International Conference on Artificial Intelligence and Statistics*, pages 4447–4455. PMLR.
- Yuntao Bai, Andy Jones, Kamal Ndousse, Amanda Askell, Anna Chen, Nova DasSarma, Dawn Drain, Stanislav Fort, Deep Ganguli, Tom Henighan, et al. 2022. Training a helpful and harmless assistant with reinforcement learning from human feedback. *arXiv preprint arXiv:2204.05862*.
- Tom Brown, Benjamin Mann, Nick Ryder, Melanie Subbiah, Jared D Kaplan, Prafulla Dhariwal, Arvind Neelakantan, Pranav Shyam, Girish Sastry, Amanda Askell, et al. 2020. Language models are few-shot learners. *Advances in neural information processing systems*, 33:1877–1901.
- Aakanksha Chowdhery, Sharan Narang, Jacob Devlin, Maarten Bosma, Gaurav Mishra, Adam Roberts, Paul Barham, Hyung Won Chung, Charles Sutton, Sebastian Gehrmann, et al. 2023. Palm: Scaling language modeling with pathways. *Journal of Machine Learning Research*, 24(240):1–113.
- Paul F Christiano, Jan Leike, Tom Brown, Miljan Martic, Shane Legg, and Dario Amodei. 2017. Deep reinforcement learning from human preferences. *Advances in neural information processing systems*, 30.
- Ganqu Cui, Lifan Yuan, Ning Ding, Guanming Yao, Bingxiang He, Wei Zhu, Yuan Ni, Guotong Xie, Ruobing Xie, Yankai Lin, et al. 2024. Ultrafeedback: Boosting language models with scaled ai feedback. In *Forty-first International Conference on Machine Learning*.
- Josef Dai, Xuehai Pan, Ruiyang Sun, Jiaming Ji, Xinbo Xu, Mickel Liu, Yizhou Wang, and Yaodong Yang. 2024. Safe RLHF: Safe reinforcement learning from human feedback. In *The Twelfth International Conference on Learning Representations*.
- Ning Ding, Yulin Chen, Bokai Xu, Yujia Qin, Shengding Hu, Zhiyuan Liu, Maosong Sun, and Bowen Zhou. 2023. Enhancing chat language models by scaling high-quality instructional conversations. In *Proceedings of the 2023 Conference on Empirical Methods in Natural Language Processing*, pages 3029–3051, Singapore. Association for Computational Linguistics.
- Iason Gabriel. 2020. Artificial intelligence, values, and alignment. *Minds and machines*, 30(3):411–437.
- Aaron Grattafiori, Abhimanyu Dubey, Abhinav Jauhri, Abhinav Pandey, Abhishek Kadian, Ahmad Al-Dahle, Aiesha Letman, Akhil Mathur, Alan Schelten, Alex Vaughan, et al. 2024. The llama 3 herd of models. *arXiv preprint arXiv:2407.21783*.
- Sam Houlston, Alizée Pace, Alexander Immer, and Gunnar Rätsch. 2024. Uncertainty-penalized direct preference optimization. *arXiv preprint arXiv:2410.20187*.
- Jiaming Ji, Donghai Hong, Borong Zhang, Boyuan Chen, Josef Dai, Boren Zheng, Tianyi Qiu, Boxun Li, and Yaodong Yang. 2024. Pku-saferlhf: Towards multi-level safety alignment for llms with human preference. *arXiv preprint arXiv:2406.15513*.

- Albert Q. Jiang, Alexandre Sablayrolles, Arthur Mensch, Chris Bamford, Devendra Singh Chaplot, Diego de las Casas, Florian Bressand, Gianna Lengyel, Guillaume Lample, Lucile Saulnier, L  lio Renard Lavaud, Marie-Anne Lachaux, Pierre Stock, Teven Le Scao, Thibaut Lavril, Thomas Wang, Timoth  e Lacroix, and William El Sayed. 2023. [Mistral 7b](#). *Preprint*, arXiv:2310.06825.
- Jongwoo Ko, Sungnyun Kim, Tianyi Chen, and Se-Young Yun. 2024. Distillm: towards streamlined distillation for large language models. In *Proceedings of the 41st International Conference on Machine Learning*, pages 24872–24895.
- Andreas K  pf, Yannic Kilcher, Dimitri von R  tte, Sotiris Anagnostidis, Zhi Rui Tam, Keith Stevens, Abdullah Barhoum, Duc Nguyen, Oliver Stanley, Rich  rd Nagyfi, et al. 2024. Openassistant conversations-democratizing large language model alignment. *Advances in Neural Information Processing Systems*, 36.
- Harrison Lee, Samrat Phatale, Hassan Mansoor, Thomas Mesnard, Johan Ferret, Kellie Ren Lu, Colton Bishop, Ethan Hall, Victor Carbune, Abhinav Rastogi, and Sushant Prakash. 2024. [RLAIF vs. RLHF: Scaling reinforcement learning from human feedback with AI feedback](#). In *Forty-first International Conference on Machine Learning*.
- Junlong Li, Fan Zhou, Shichao Sun, Yikai Zhang, Hai Zhao, and Pengfei Liu. 2024a. [Dissecting human and LLM preferences](#). In *Proceedings of the 62nd Annual Meeting of the Association for Computational Linguistics (Volume 1: Long Papers)*, pages 1790–1811, Bangkok, Thailand. Association for Computational Linguistics.
- Lei Li, Zhihui Xie, Mukai Li, Shunian Chen, Peiyi Wang, Liang Chen, Yazheng Yang, Benyou Wang, Lingpeng Kong, and Qi Liu. 2024b. [Vlfeedback: A large-scale ai feedback dataset for large vision-language models alignment](#). In *Proceedings of the 2024 Conference on Empirical Methods in Natural Language Processing*, pages 6227–6246.
- Yu Meng, Mengzhou Xia, and Danqi Chen. 2024. [SimPO: Simple preference optimization with a reference-free reward](#). In *The Thirty-eighth Annual Conference on Neural Information Processing Systems*.
- Reiichiro Nakano, Jacob Hilton, Suchir Balaji, Jeff Wu, Long Ouyang, Christina Kim, Christopher Hesse, Shantanu Jain, Vineet Kosaraju, William Saunders, et al. 2021. [Webgpt: Browser-assisted question-answering with human feedback](#). *arXiv preprint arXiv:2112.09332*.
- Long Ouyang, Jeffrey Wu, Xu Jiang, Diogo Almeida, Carroll Wainwright, Pamela Mishkin, Chong Zhang, Sandhini Agarwal, Katarina Slama, Alex Ray, et al. 2022. Training language models to follow instructions with human feedback. *Advances in neural information processing systems*, 35:27730–27744.
- Rafael Rafailov, Archit Sharma, Eric Mitchell, Christopher D Manning, Stefano Ermon, and Chelsea Finn. 2024. Direct preference optimization: Your language model is secretly a reward model. *Advances in Neural Information Processing Systems*, 36.
- John Schulman, Filip Wolski, Prafulla Dhariwal, Alec Radford, and Oleg Klimov. 2017. [Proximal policy optimization algorithms](#). *Preprint*, arXiv:1707.06347.
- Nisan Stiennon, Long Ouyang, Jeffrey Wu, Daniel Ziegler, Ryan Lowe, Chelsea Voss, Alec Radford, Dario Amodei, and Paul F Christiano. 2020. Learning to summarize with human feedback. *Advances in Neural Information Processing Systems*, 33:3008–3021.
- Zhiqing Sun, Yikang Shen, Qinhong Zhou, Hongxin Zhang, Zhenfang Chen, David Cox, Yiming Yang, and Chuang Gan. 2024. Principle-driven self-alignment of language models from scratch with minimal human supervision. *Advances in Neural Information Processing Systems*, 36.
- Swabha Swayamdipta, Roy Schwartz, Nicholas Lourie, Yizhong Wang, Hannaneh Hajishirzi, Noah A Smith, and Yejin Choi. 2020. Dataset cartography: Mapping and diagnosing datasets with training dynamics. In *Proceedings of the 2020 Conference on Empirical Methods in Natural Language Processing (EMNLP)*, pages 9275–9293.
- Hugo Touvron, Louis Martin, Kevin Stone, Peter Albert, Amjad Almahairi, Yasmine Babaei, Nikolay Bashlykov, Soumya Batra, Prajjwal Bhargava, Shruti Bhosale, et al. 2023. [Llama 2: Open foundation and fine-tuned chat models](#). *arXiv preprint arXiv:2307.09288*.
- Alexander Wettig, Aatmik Gupta, Saumya Malik, and Danqi Chen. 2024. [Qurating: Selecting high-quality data for training language models](#). In *Forty-first International Conference on Machine Learning*.
- Junkang Wu, Yuexiang Xie, Zhengyi Yang, Jiancan Wu, Jinyang Gao, Bolin Ding, Xiang Wang, and Xiangnan He. 2024. [\\$beta\\$-dpo: Direct preference optimization with dynamic \\$beta\\$](#). *Advances in Neural Information Processing Systems*, 37:129944–129966.
- Zequ Wu, Yushi Hu, Weijia Shi, Nouha Dziri, Alane Suhr, Prithviraj Ammanabrolu, Noah A Smith, Mari Ostendorf, and Hannaneh Hajishirzi. 2023. Fine-grained human feedback gives better rewards for language model training. *Advances in Neural Information Processing Systems*, 36:59008–59033.
- Sang Michael Xie, Shibani Santurkar, Tengyu Ma, and Percy Liang. 2023. [Data selection for language models via importance resampling](#). In *Thirty-seventh Conference on Neural Information Processing Systems*.
- Can Xu, Qingfeng Sun, Kai Zheng, Xiubo Geng, Pu Zhao, Jiazhan Feng, Chongyong Tao, Qingwei

Lin, and Daxin Jiang. 2024. Wizardlm: Empowering large pre-trained language models to follow complex instructions. In *The Twelfth International Conference on Learning Representations*.

Sen Yang, Leyang Cui, Deng Cai, Xinting Huang, Shuming Shi, and Wai Lam. 2024. Not all preference pairs are created equal: A recipe for annotation-efficient iterative preference learning. In *Findings of the Association for Computational Linguistics: EMNLP 2024*, pages 6549–6561.

Tianyu Yu, Haoye Zhang, Yuan Yao, Yunkai Dang, Da Chen, Xiaoman Lu, Ganqu Cui, Taiwen He, Zhiyuan Liu, Tat-Seng Chua, et al. 2024. Rlaif-v: Aligning mllms through open-source ai feedback for super gpt-4v trustworthiness. *arXiv preprint arXiv:2405.17220*.

Lianmin Zheng, Wei-Lin Chiang, Ying Sheng, Siyuan Zhuang, Zhanghao Wu, Yonghao Zhuang, Zi Lin, Zhuohan Li, Dacheng Li, Eric Xing, et al. 2023. Judging llm-as-a-judge with mt-bench and chatbot arena. *Advances in Neural Information Processing Systems*, 36:46595–46623.

Appendix

A Supplemental Material

A.1 Datasets

This appendix provides a detailed description of the datasets used in our experiments. We conduct experiments on a large-scale dataset: UltraFeedback (Cui et al., 2024). UltraFeedback datasets belong to the AI-feedback category, where AI annotations replace human evaluations. Specifically, GPT-4 is utilized to quantitatively assess response quality.

UltraFeedback UltraFeedback is constructed by selecting instructions from multiple datasets and defining 17 model pools. For each instruction, four models are randomly chosen to generate responses. This process generates a total of 255,864 completions, each of which GPT-4 evaluates based on four criteria: Instruction-Following, Truthfulness, Honesty, and Helpfulness. These evaluation scores are provided as scalar values, and we utilize the average score across the four criteria as a fine-grained metric.

A.2 Benchmarks

To assess LLM alignment, we employ the following alignment benchmarks:

- MT-Bench (Zheng et al., 2023) evaluates a chatbot’s ability to engage in multi-turn conversations and follow instructions. It measures how well a model maintains natural dialogue while accurately executing given instructions. We use `llm-judge` (Zheng et al., 2023) to assess model response quality. The evaluation is conducted using GPT-4o-2024-11-20 as the judging model, generating performance scores for responses. Each evaluation sample consists of two turns of conversation, and we report the average score (single score) across the two responses. To compare relative performance, we additionally conduct pairwise comparisons (win rate) between model-generated responses and those from GPT-3.5-turbo. For each prompt, both responses are rated by GPT-4o-2024-11-20, and a win/lose/tie label is assigned based on which response is preferred.
- Evol-Instruct (Xu et al., 2024) addresses the limitations of existing benchmarks that over-represent relatively simple instructions. It

provides a more balanced benchmark dataset by leveraging LLMs to automatically generate instruction data with diverse levels of complexity. Evaluation on Evol-Instruct adopts the same automatic judgment framework as MT-Bench, using `llm-judge` with GPT-4o-2024-11-20 as the evaluator. For each instruction, the judge compares responses generated by the target model and GPT-3.5-turbo, assigns win/lose/tie labels, and evaluates the quality of each response to produce numerical scores. These results are used to compute both the win rate and the single score.

A.3 Experimental Settings

We train the LLaMA-3-8b and Mistral-7b supervised fine-tuned models on the UltraFeedback dataset using DPO and SimPO methods (Touvron et al., 2023). For LLaMA-3-8b, DPO training is conducted with a beta value of 0.01 and learning rate of $5e-7$, while SimPO training uses beta values of 2.0, gamma-beta ratio of 0.5, and learning rate of $6e-7$. SimPO achieves the best performance across all benchmarks. For Mistral-7b, DPO training is performed with beta values of 0.01 and learning rate of $5e-7$, whereas SimPO uses a beta of 2.0 and a gamma-beta ratio of 0.8, and learning rate of $3e-7$. DPO reports the highest performance in this setting. We adopted the hyperparameter configuration from Meng et al. (2024). All training is conducted on four RTX A6000 ada GPUs.

Model (Method)	β	γ/β	lr
LLaMA-3-8b (DPO)	0.01	-	$1e-7$
Mistral-7b (DPO)	0.01	-	$5e-7$
LLaMA-3-8b (SimPO)	2.0	0.5	$6e-7$
Mistral-7b (SimPO)	2.0	0.8	$3e-7$

Table 4: Hyperparameter used in DPO and SimPO training.

B Preference Alignment by SimPO

SimPO Gradient Analysis. The gradient of the SimPO loss function $\mathcal{L}_{\text{SimPO}}$ can be expressed as follows (Meng et al., 2024).

$$\nabla_{\theta} \mathcal{L}_{\text{SimPO}}(\pi_{\theta}) = -\beta \mathbb{E}_{(x, y_w, y_l) \sim \mathcal{D}} [\sigma(-\rho_{\theta}) \cdot d_{\theta}]$$

where

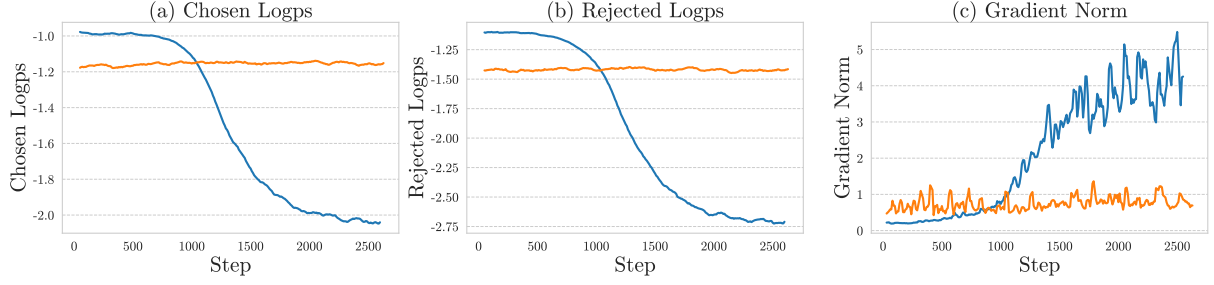


Figure 6: Training dynamics of SimPO on High Average and Low Average subsets—(a) log-probabilities of chosen responses, (b) log-probabilities of rejected responses, and (c) gradient norm over training steps. The colored lines represent data selection strategies: **High Average** (blue), **Low Average** (orange).

$$\rho_\theta = \left(\frac{\beta}{|y_w|} \log \pi_\theta(y_w | x) - \frac{\beta}{|y_l|} \log \pi_\theta(y_l | x) - \gamma \right)$$

$$d_\theta = \frac{1}{|y_w|} \nabla_\theta \log \pi_\theta(y_w | x) - \frac{1}{|y_l|} \nabla_\theta \log \pi_\theta(y_l | x)$$

- In $\sigma(-\rho_\theta)$, ρ_θ denotes the difference in log probabilities between the chosen and rejected responses. When ρ_θ is small—i.e., when the model has similar confidence in both choices— $\sigma(-\rho_\theta)$ takes a large value. Conversely, when ρ_θ is large, $\sigma(-\rho_\theta)$ approaches zero.
- This indicates that samples where the model is less confident in preferring the chosen response over the rejected one contribute more to the loss and result in larger gradient updates. Empirically, it has been observed that for near-deterministic preference pairs (e.g., with probabilities close to 0 or 1), the gradient contribution becomes negligible, potentially limiting SimPO’s effectiveness in such scenarios (Azar et al., 2024).
- d_θ corresponds to the margin of the policy’s log probability gradient. It is well known that lower probability values result in larger gradient magnitudes (Ko et al., 2024). Specifically, for small values of $\log \pi_\theta(y | x)$, the gradient $\nabla_\theta \log \pi_\theta(y | x)$ becomes large. As a result, in the SimPO objective, samples with very low policy probabilities $\log \pi_\theta(y | x)$ can induce excessively large gradients. This may lead to unstable training behavior due to over-amplified updates in response to small preference margins (Houliston et al., 2024).

Analysis on experiment results. We analyze the impact of these three data regions on the SimPO

loss gradient in Figure 6. In the **HighAvg** region, due to low variance and high average preference scores, both the win and loss samples tend to receive high log probability estimates. In contrast, the **LowAvg** region exhibits low variance and low average scores, resulting in low log probabilities for both win and loss samples. As shown in Figures 6(a) and 6(b), both the chosen and rejected responses exhibit higher initial log probabilities in the **HighAvg** region. This indicates that the generation probabilities for these instances are relatively higher compared to those in the **LowAvg** region. Consequently, the gradient norm behavior observed in Figure 6(c) differs accordingly: in the **HighAvg** region, the gradients at the early stages of training are smaller and more stable, whereas in the **LowAvg** region, the gradients tend to be larger and more volatile during early training.

C Correlation Hexbin Plot

We construct the data map using the UltraFeedback dataset, dividing it into three subsets—High Variance, High Average, and Low Average—based on the proposed criteria. For each subset, we compute the variance and average from the feedback scores \mathcal{F} and visualize the resulting structure. Figure 7 illustrates the distribution of each subset. The High Variance group is characterized by a larger number of samples with relatively high variance when calculated using the actual preference scores. In the High Average group, most data points exhibit an average score of approximately 4.5 or higher, with variance values concentrated near zero. In contrast, the Low Average group displays a distribution skewed toward lower average scores, and the overall mean is noticeably lower than that of the High Average group. This visualization demonstrates that the proposed data partitioning criteria effectively capture the statistical characteristics of

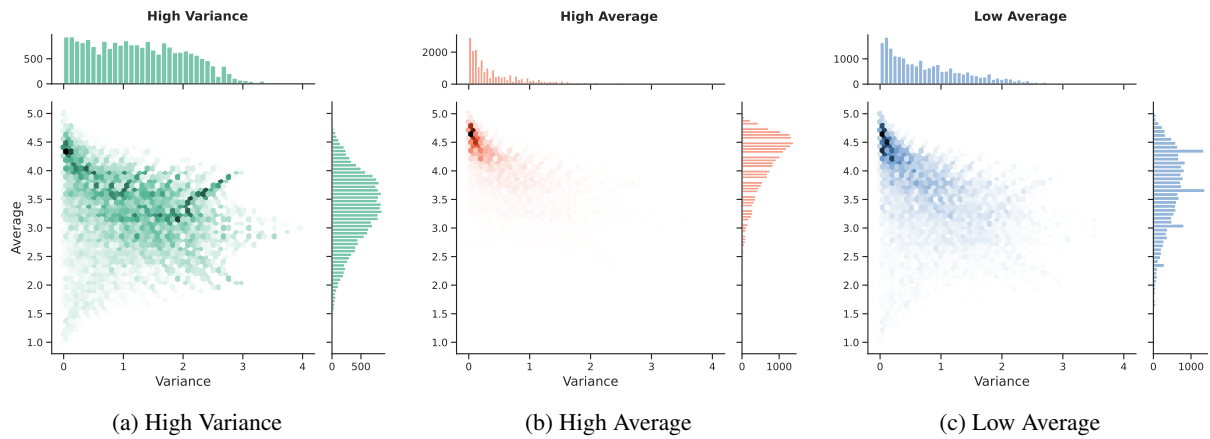


Figure 7: Hexbin jointplots for High Variance, High Average and Low Average.

the actual preference scores.

D Case Study

Table 5 presents a case study comparing model responses across three data regions: *High Average*, *High Variance*, and *Low Average*. Given a prompt requiring grammatical correction, the High-Avg response provides a clear and coherent revision with a high score of 9. In contrast, both High-Var and LowAvg responses receive lower scores of 4 due to ambiguity, insufficient grammatical corrections, and failure to follow the instruction precisely. These responses are also less aligned with human preferences in terms of clarity and task relevance. Specifically, these responses fail to clarify the speaker’s intent and do not fully resolve key errors in the original text.

Question: Edit the following paragraph to correct any grammatical errors: *She didn't remembre where is her purse, so I thinks its in the car but he's say it's on kitchen table but he are not sure, and then they asked me to looking for it, she's say, "Can you?", and I responds with, "Maybe, but ain't no sure," and he not heard me, and, "What?", he asks, "Did you found it?"*

Region	Model Response	Score
HighAvg.	She couldn't remember where her purse was, so I suggested that it might be in the car. However, he said it was on the kitchen table but wasn't sure. They asked me to help find it, and she said, "Can you?" I replied, "I'm not sure, but I'll try," and he didn't hear me. He asked, "Did you find it?" "No, I'm sorry," I answered.	9
HighVar.	It is not clear from the sentence "she's say, 'Can you?' and I responds with, 'Maybe, but ain't no sure,'" what the speaker is responding to. It could be interpreted as a response to the question "Can you?" or to "Did you found it?" It is also unclear if the speaker is responding to a question being asked by another person or is responding to their own thoughts. To correct these grammatical errors, the sentence could be rewritten as: "She asked me, 'Can you find my purse?' and I replied, 'I'm not sure, but I'll try my best.'"	4
LowAvg.	It is not clear from the sentence "she's say, 'Can you?' and I responds with, 'Maybe, but ain't no sure,'" what the speaker is responding to. It could be interpreted as a response to the question "Can you?" or to "Did you found it?" It would be helpful to clarify which question the speaker is responding to. Additionally, the sentence "he not heard me" should be changed to "he didn't hear me" for proper grammar. Finally, the sentence "and, 'What?', is not necessary as it is not a complete sentence.	4

Table 5: Case study from MT-Bench evaluating Llama3-8B model fine-tuned via SimPO. Responses from different data regions (High Average, High Variance, Low Average) are compared in terms of grammatical correction quality.